

Key Technologies to enable Terabit-scale Digital Radio-over-Fiber Systems

Xiaodan Pang^{*a,b}, Lu Zhang^{a,d}, Oskars Ozolins^{c,a}, Aleksejs Udalcovs^c, Rui Lin^a, Richard Schats^a, Shilin Xiao^d, Weisheng Hu^d, Sergei Popov^a, Gunnar Jacobsen^c, Jiajia Chen^a

^aKTH Royal Institute of Technology, Electrum 229, Kista, Sweden, SE-164 40;

^bInfinera, Fredsborgsgatan 24, Stockholm, Sweden SE-117 43;

^cRISE Research Institute of Sweden, Isafjordsgatan 22, Kista, Sweden, SE-164 40;

^dState Key Laboratory of Advanced Optical Communication System and Networks, Shanghai Jiao Tong University, Shanghai, China, 200240

ABSTRACT

With the approach of the 5G era, stringent requirements are imposed on the data transport solutions, including both of the supported transmission reach and the capacity. Radio-over-fiber technologies are considered to be promising candidates to cope with both aspects, owing to the low-loss and broad-bandwidth nature of the optical fibers. Meanwhile with such optical transport solutions, signals can be collected from the distributed remote radio sites and processed in a centralized manner. In this report, we target on the digital radio-over-fiber systems, and discuss about several key technologies, focusing on the aspects of coding and transmission, which could potentially enable terabit-scale data transport.

Keywords: Digital radio-over-fiber, fiber optics communications, radio frequency photonics, modulation, coding

1. INTRODUCTION

Driven by the development of 5G applications and technologies, such as the massive multiple input multiple output (MIMO) technique, there is an exponential increase of traffic demand in the mobile fronthaul systems [1] to delivery large amount of aggregated radio signals. As a result, improving the mobile fronthaul system spectral efficiency thus the system throughput is of great importance to meet the existing challenges.

Optical fiber is preferred as a promising media to deliver radio signals thanks to its advantages of large operational bandwidth and high reliability. Furthermore, radio-over-fiber (RoF) system [2] is an attractive technology because of its inherent merits in transmission reach and speed, as well as the centralized processing capability, which leads to low cost and high energy efficiency for networking management. Considering the RoF systems for the mobile fronthaul scenario, both analog and digital configurations have been widely analyzed [2]. Although the analog RoF systems show advantages like high spectral efficiency, it is significantly affected by the nonlinear distortions from the optoelectronic devices as well as from the fiber link. As a result, the transmission quality and distance are severely influenced, difficult to meet the specifications for high-speed applications, such as the 5G new-radio (NR) [3]. In contrast, the digital RoF systems are more immune to the nonlinear channel distortions, allowing for a longer transmission distance and better transmission performance comparing to its analog counterpart.

In 4G (LTE) and 5G communication protocols, the pulse coding based common public radio interface (CPRI) protocol [4] and the Option 8 based enhanced CPRI (eCPRI) protocol [4] transmit digitized analog signal between central units and remote radio units (RRUs). However, the pulse coding based digital RoF system scheme requires high data rate due to the large number of quantization bits (QBs). For instance, a site with the configuration of 25 5G-NR channels (with the 15 QBs, sampling rate of 122.88-MSa/s, 64B/66B line code, and 1/16 MIMO processing overhead) requires a total link rate of 101.38-Gbps ($122.88\text{-MSa/s} \times 25 \times 2 \times 15\text{bits} \times 16/15 \times 66/64$). To address the capacity crunch of digital RoF system, there are mainly two research focuses: 1) increasing the RoF system capacity with high speed transmission

*xiaodan@kth.se

scheme, e.g. coherent transmission [5-6]; 2) improving the spectral efficiency using effective compression coding [7-13]. However, 5G-NR, where full dimension massive-MIMO is expected to implement active-phased-array-antennas with the array size of 128 and possibly beyond, could make the existing digital RoF solutions not sufficient to meet the capacity requirement.

In this paper, we propose adopting the “parallelism” concept in a novel digital RoF system architecture with multi-core fiber (MCF) and self-homodyne coherent detection, namely digital radio-over MCF (RoMCF) system. Compared with common digital RoF system, the proposed digital RoMCF system utilizes MCF to deliver digitized radio signals, which increases the transported data rate by scaling up the lane count per fiber. Besides, by transmitting local oscillator (LO) delivered through one core of the MCF, the proposed RoMCF system can effectively support self-homodyne coherent detection, which can increase the lane rate per core. To further improve the RoMCF system spectral efficiency, source coding schemes are introduced for effective quantization of analog radio signals. In the lossy source coding scheme, the differential coding and the vector coding are employed and compared. In the lossless source coding scheme, the Huffman coding and the arithmetic coding are employed and compared. Proof-of-concept demonstration of the proposed digital RoMCF system is carried out with 28-Gbaud self-homodyne digital radio-over-33.6km-7-core-fiber. Combining with proper coding techniques, the achieved QAM orders vary from 4 to 4096, which can support various types of radio services. The aggregated 5G-NR channel number reaches 460 with 4096-QAM and 1285 with 4-QAM, respectively. The corresponding CPRI-equivalent rates vary from 1.56-Tbps to 5.21-Tbps.

2. DIGITAL RADIO-OVER MULTI-CORE FIBER SYSTEM

Figure 1 shows the proposed digital RoMCF system architecture. The signals from the central unit are digitalized with the source coding modules and arranged in time domain frames, before carrier aggregation through time domain multiplexing (TDM). The source coding module consists of lossy coding and lossless coding schemes. After aggregation, the digital I/Q signals are mapped to optical signal formats. After digital-to-analog converter, the signals are loaded to the optical I/Q modulators. A laser output signal is split by an optical splitter. Then, one branch is delivered directly through one core of the MCF and used as the LO for self-homodyne at the receiver side, and the other $N-1$ branches are sent to the optical I/Q modulators.

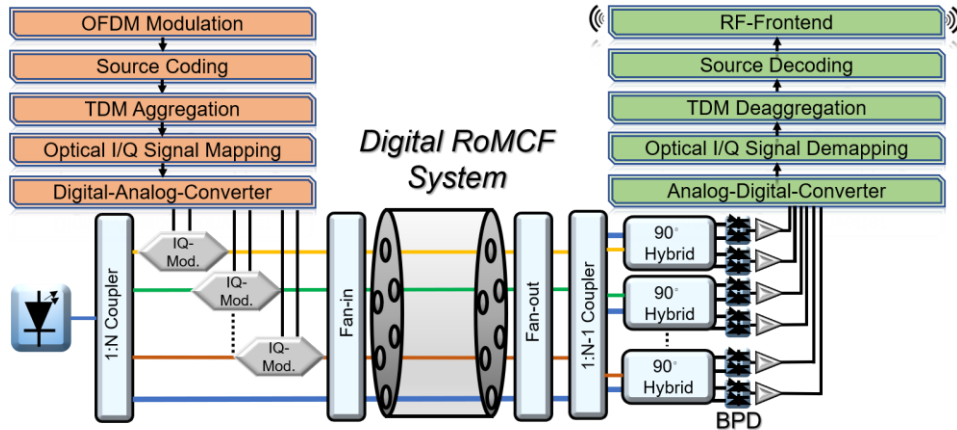


Fig. 1. Architecture of proposed digital RoMCF system.

At the remote site, the digitized radio signals and the LO after MCF transmission are de-coupled by the fan-out module and received by coherent receivers. After analog-to-digital conversion, the signal is demodulated to the TDM framed signals. Then, the signal is de-aggregated by time domain de-framing, and the separated frames are passed to the designated source decoding module. Subsequently, the digital signals are converted to analog by the source decoding module and modulated to different antenna-carriers by radio frequency (RF) frontend. Regarding the uplink transmission, it follows the same operation principle, but in the opposite order.

3. COMPRESSED QUANTIZATION

The main challenge of the digital RoF system is the sacrificed spectral efficiency from high QBs of digitalization of the analog radio signals. This is an important aspect to study in our proposed digital RoMCF system. This section will

discuss compressed quantization methods to reduce the number of QBs and increase the spectral efficiency of digital RoF systems.

3.1 Lossy coding schemes

The analog radio signals mostly adopt multicarrier modulation formats at the air interface, where the orthogonal frequency division modulation (OFDM) signal format is widely adopted. In the OFDM modulation, only a fraction of the subcarriers are loaded with data and the rest are left blank as the guard band. As a result, the neighboring samples of the analog signals exhibit strong sample-to-sample correlation properties. Such correlation properties can be used to reduce the redundancy during quantization of the analog signals. Lossy source coding is used to remove the redundancy during quantization of the analog signals and reduce the number of QBs. The ‘lossy’ means the quantization process is not perfectly revertible and there is quantization noise, which is inevitable during digitization. In the proposed digital RoMCF system, we consider two types of lossy source coding schemes, namely scalar coding and vector coding, and differential coding is implemented as the instance of scalar coding.

Differential coding utilizes the correlation between the neighboring samples of the analog symbols for getting a high signal-to-quantization noise ratio and a low number of the required QBs.

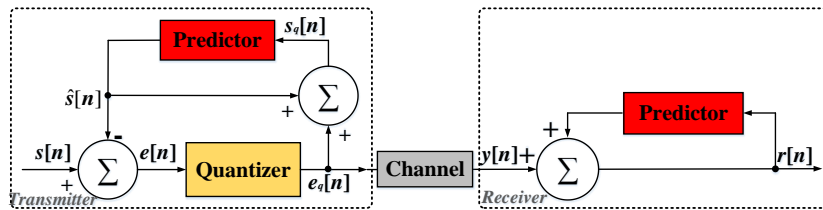


Fig. 2. Diagram for the differential coding with a linear predictor [8].

Figure 2 illustrates differential coding-based quantization scheme with a linear predictor [8]. At the transmitter, the real and imaginary (I and Q) components of each baseband analog signal $s(t)$ is sampled at rate $f_s=1/T_s$, to produce samples $s[n] = s(t)|_{t=nT_s}$, $n=1, \dots, N$, where N is the symbol length, and T_s is the sampling interval. The linear predictor predicts the samples $s[n]$, and the quantization is carried out based on the sampled signal $s[n]$ and its prediction $\hat{s}[n]$. Meanwhile, the difference between the sampled signal and the predicted signal can be optimized in order to minimize the quantization noise and reduce the number of quantization bits. The coding is carried out by quantizing the difference between the current sample $s[n]$ and its predicted value $\hat{s}[n]$. Least-mean square (LMS) algorithm is used to get the optimal predictor coefficient [8]. For prediction, at the beginning of the analog radio signals (containing several symbols), the first trunk of samples are selected as training data. The samples are then encoded and decoded without loss of information. Then, the encoding and decoding of the next samples are performed based on the prediction coefficients obtained from the training data, the optimized quantization levels calculated by QBs and the differential signal of the training data. In the implementation [8], Levinson-Durbin algorithm is used to get optimized coefficient, and Lloyd algorithm is used to optimize the codebooks using the predictive errors produced by Levinson-Durbin algorithm.

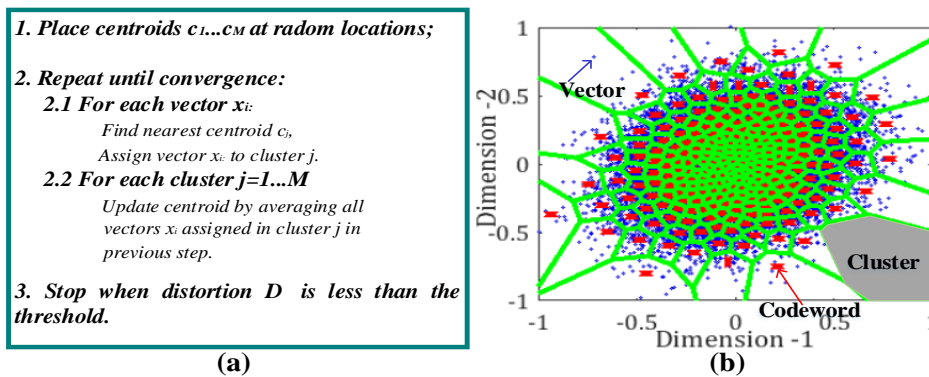


Fig.3. (a) schematic diagram of multi-dimensional quantization scheme, (b) example of 2-D quantization [11].

Vector coding scheme also utilizes the correlation between neighboring samples of analog symbols, it uses the concept of k-means clustering algorithm to do the quantization in a high dimension. The k-means clustering algorithm in the quantization scheme is shown in Fig. 3 (a). At the transmitter, the discrete time domain I and Q signals $\{real(s_i), imag(s_i)|i=1, \dots, L\}$ are converted into vectors by grouping n samples into n -D vectors (e.g. $x_i = \{real(s_i), imag(s_i) | i, j \in [1, L]\}$ forms a 2-D vector). In the k-means clustering algorithm, the M centroids $\{c_1, \dots, c_M\}$ are generated randomly at the initial stage. Then, in every loop, the vector x_i finds nearest centroid c_j by calculating the Euclidian distance between x_i and c_j . For each cluster, a new centroid $c_j = \text{mean}(x_i | x_i \rightarrow c_j)$ is obtained by averaging all samples assigned in cluster j in the previous step. The loop is terminated when the distortion $D = \text{sum}(x_i - (c_i \rightarrow x_i))$ is less than predefined threshold. The k-means clustering algorithm produces M clusters, which correspond to M quantization levels and $\log_2(M)$ quantization bits, the quantization bits per sample is $\log_2(M)/n$. As shown in Fig. 3 (b), it is an example of 2-D clustering of OFDM signal. For each vector, it falls into one cluster with a typical codeword, and then it is quantized as the corresponding codeword. The clusters are not evenly distributed due to high peak-to-average ratio (PAPR) of the OFDM signals, and it is denser with a lower amplitude region.

3.2 Lossless coding schemes

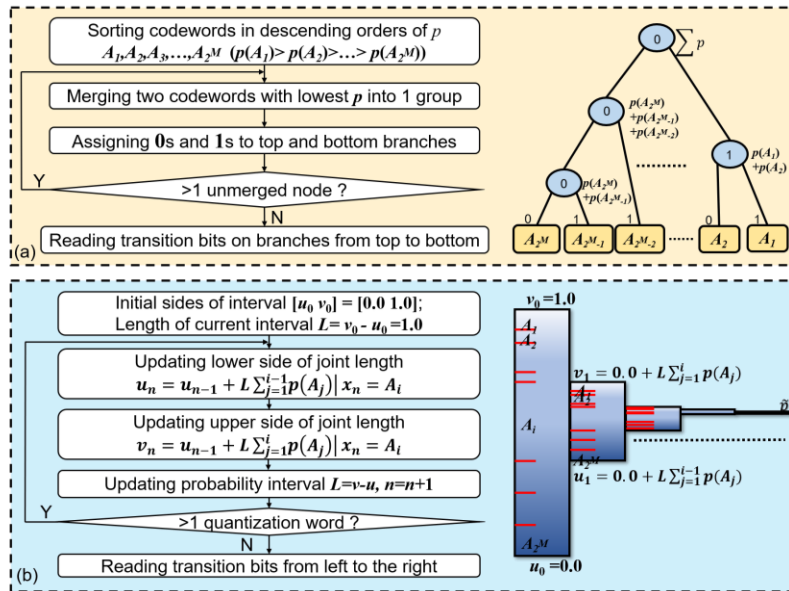


Fig. 4. Lossless coding scheme with a) Huffman coding and b) arithmetic coding.

At the air interface of 5G-NR, the OFDM signals often show a high PAPR. In the digital mobile fronthaul, most of the quantized signals, i.e., codewords, need to be distributed in the low-amplitude region and very few codewords are required in the high-amplitude region. It causes entropy redundancy, since all codewords share the same number of QBs. Lossless source coding is promising to reduce such entropy redundancy. The idea of lossless source coding is very simple, where the codewords occurred more frequently are implemented by shorter codes while the codewords occurred less frequently are implemented by longer codes. We introduce both Huffman coding (Fig. 4a) and arithmetic coding (Fig. 4b) for compressed quantization in the proposed RoMCF system.

For Huffman coding, the codewords are sorted by their probabilities of occurrences in descending order. Assuming in total M number of QBs, there are 2^M codewords $\{A_1, A_2, \dots, A_{2^M}, p(A_1) > p(A_2) > \dots > p(A_{2^M})\}$, where $p(A_i)$ represents the probability that codeword A_i occurs. Two nodes with the lowest probabilities are chosen and assigned with value 0 and 1, respectively. Then these two nodes are merged into a new node with the weight as sum of weight of its two child nodes. If there is still unmerged node, the algorithm continues to find two nodes with the lowest weight, which are assigned value 0 and 1, respectively, and then merged to a new node. Finally, for every codeword, the coded bits are read from the root to the leaf node.

Although the Huffman coding nearly approaches the entropy of quantization, the code length for each codeword should be integer, which produces rounding errors. Arithmetic coding overcomes such problem. Fig. 4b shows how to construct the arithmetic coding scheme. In the initial stage, all possible codewords are in the range $[u_0, v_0)$, where $u_0=0.0$, and $v_0=1.0$. In every iteration, a new quantization word $x_n=A_i$ with a cumulative probability range $[low_i, high_i]$ is handled,

where $low_i = \sum(p(A_1) \rightarrow p(A_{i-1}))$ and $high_i = \sum(p(A_1) \rightarrow p(A_i))$, and the range $[u_n, v_n)$ is updated accordingly, where $u_n = u_{n-1} + (v_{n-1} - u_{n-1}) * low_i$ and $v_n = u_{n-1} + (v_{n-1} - u_{n-1}) * high_i$. Finally, when all quantization words are handled, a probability $p_0 = (u_n + v_n) / 2$ is selected. For example, if $p_0 = 0.6640625_{10} = 0.1010101_2$, and the entire codeword is 1010101.

4. PROOF-OF-CONCEPT EXPERIMENT AND RESULTS

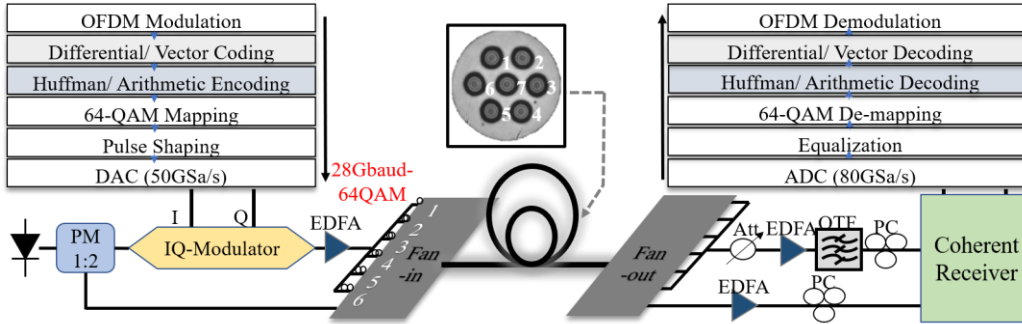


Fig. 5. Proof-of-concept experimental setup.

To demonstrate the feasibility of the proposed RoMCF system and the validity of the key technologies in the previous section, a proof-of-concept RoMCF experiment is carried out. The experimental setup is shown in Fig. 5. Self-homodyne coherent detection scheme with a 7-core fiber is adopted for increasing the system data rate. Thanks to such self-homodyne link configuration [14], the merits of coherent transmission system, such as high spectral efficiency and high sensitivity can be realized in our proposed RoMCF system.

In our experiment, OFDM signal and 2048-IFFT points are used. The sampling rate per OFDM symbol is 122.88-MSa/s with the bandwidth of 100-MHz. At the transmitter side, the quantization sequence is generated and encoded with the proposed lossy and lossless coding schemes. They are mapped to 64-QAM constellations followed by Nyquist pulse shaping. An IQ-modulator is driven by the 64-QAM signals transmitted from the two outputs of a digital to analog converter (DAC, 50-GSa/s). The lightwave from a semiconductor laser is split using a polarization maintaining 50:50 splitter. One is used as the transmitter laser, and the other one transmitted through one core of the MCF is used as the LO at the receiver side. The output optical signal from the IQ modulator is amplified by an erbium-doped fiber amplifier (EDFA), divided into 6 branches using a power splitter, decorrelated, and then coupled into the remaining 6 cores of the low-crosstalk 7-core MCF via a fan-in device. After 33.6-km MCF, the channels are demultiplexed by a fan-out. A noise loading module consisting of an optical attenuator and an EDFA, is placed to adjust a channel optical signal-to-noise ratio (OSNR). Finally, the signals are coherently detected and sampled by an analog to digital converter (ADC, 80-GSa/s). For all the cores, we have achieved error-free 64-QAM transmissions after hard-decision forward error correction (HD-FEC) threshold.

| QAM Orders | Aggregated 5G-NR channels | | | | | | Equivalent CPRI rates (Tbps) | | | | | |
|------------|---------------------------|--------------|-------------|-----------|-----------|-----------|------------------------------|--------------|-------------|-----------|-----------|-----------|
| | Diff. | Diff. +Huff. | Diff. +Ari. | Vec. (1D) | Vec. (2D) | Vec. (3D) | Diff. | Diff. +Huff. | Diff. +Ari. | Vec. (1D) | Vec. (2D) | Vec. (3D) |
| 4 | 1156 | 1205 | 1285 | 867 | 1156 | 1156 | 4.69 | 4.89 | 5.21 | 3.52 | 4.69 | 4.69 |
| 16 | 867 | 932 | 973 | 694 | 867 | 867 | 3.52 | 3.78 | 3.95 | 2.81 | 3.52 | 3.52 |
| 64 | 694 | 848 | 868 | 694 | 694 | 694 | 2.81 | 3.44 | 3.52 | 2.81 | 2.81 | 2.81 |
| 256 | 495 | 613 | 629 | 578 | 578 | 578 | 2.01 | 2.49 | 2.55 | 2.34 | 2.34 | 2.34 |
| 1024 | 433 | 525 | 528 | 433 | 433 | 433 | 1.76 | 2.13 | 2.14 | 1.76 | 1.76 | 1.76 |
| 4096 | 385 | 455 | 460 | 385 | 385 | 385 | 1.56 | 1.84 | 1.87 | 1.56 | 1.56 | 1.56 |

Table 1. Experimental demonstrated aggregated 5G-NR channels and the equivalent CPRI rates (sampling rate of 122.88 MSa/s, 64B/66B line code, and 1/16 processing overhead).

The aggregated 5G-NR channels and the equivalent CPRI rates are summarized in Table 1. The codewords after differential coding fit the Gaussian distribution and the codewords in the low-amplitude region occur more frequently. Comparatively, the quantization codewords after vector coding fit the uniform distribution and the codewords in the low-amplitude region and high-amplitude region occurs with the same frequency. Thus, the vector coding has another merit compared with the differential coding, shown in its adaption to high PAPR to analog radio signals like OFDM. As a

result, lossless coding could theoretically improve the performance of differential coding while could not improve vector coding [15-16]. Finally, the supported QAM orders vary from 4 to 4096, which can support various types of radio services, and the thresholds of different modulation orders are referred to 3GPP standard (3GPP TS 36.104 V12.6.0). The aggregated 5G-NR channel number reaches 1285-ch with QAM order of 4 and reaches 460-ch with QAM order of 4096. The equivalent CPRI rates vary from 1.56-Tbps to 5.21-Tbps. Although differential coding and lossless coding achieve better performance comparing to the vector coding, it is at the expense of higher complexity.

ACKNOWLEDGEMENTS

This work was partly supported by the EU H2020 MCSA-IF Project NEWMAN (#752826), Swedish Research Council (VR), the Swedish Foundation for Strategic Research (SSF), Göran Gustafsson Foundation, the Swedish ICT-TNG, VINNOVA funded SENDATE-EXTEND and SENDATE-FICUS, National Natural Science Foundation of China (#61331010, 61722108, 61775137, 61671212), SJTU State Key Laboratory of Advanced Optical Communication System and Networks Open project 2018GZKF03001.

REFERENCES

- [1] Pfeiffer, T., "Next generation mobile fronthaul architectures," Proc. OFC, M2J.7, (2015).
- [2] ITU-T G-series Recommendations – Supplement 55, "Radio-over-fibre (RoF) technologies and their applications," 2015.
- [3] Minokuchi, A., Isobe, S., Takahashi, H., and Nagata, S., "5G Standardization Trends at 3GPP," 2018.
- [4] www.cpri.info
- [5] Xu, M., Jia, Z., Wang, J., Campos, L. A., and Chang, G. K., "A Novel Data-Compression Technology for Digital Mobile Fronthaul with Lloyd Algorithm and Differential Coding," Proc. OFC, Tu2K.2, (2018).
- [6] Zhang, L., Udalcovs, A., Lin, R., Ozolins, O., Pang, X., Gan, L., Schatz, R., Djupsjöbacka, A., Mårtensson, J., Tang, M., Fu, S., Liu, D., Tong, W., Popov, S., Jacobsen, G., Hu, W., Xiao, S. and Chen, J., "Digital Radio-over-Multicore-Fiber System with Self-Homodyne Coherent Detection and Entropy Coding for Mobile Fronthaul," Proc. ECOC, Th2.66, (2018).
- [7] Wang, J., Yu, Z., Ying, K., Zhang, J., Lu, F., Xu, M., Cheng, L., Ma, X., and Chang, G. K., "Digital Mobile Fronthaul Based on Delta-Sigma Modulation for 32 LTE Carrier Aggregation and FBMC Signals," J. Opt. Commun. Netw. 9(2), A233–A244, (2017).
- [8] Zhang, L., Pang, X., Ozolins, O., Udalcovs, A., Schatz, R., U. Westergren, Jacobsen, G., Popov, S., L. Wosinska, Hu, W., Xiao, S., and Chen, J., "Digital mobile fronthaul employing differential pulse code modulation with suppressed quantization noise," Opt. Express 25(25), 31921–31936 (2017).
- [9] Zhang, L., Pang, X., Ozolins, O., Udalcovs, A., Schatz, R., U. Westergren, Jacobsen, G., Popov, S., Xiao, S. and Chen, J., "15-Gbaud PAM4 Digital Mobile Fronthaul with Enhanced Differential Pulse Coding Modulation supporting 122 LTE-A Channels with up to 4096QAM", Proc. ECOC, W.2.B.6, (2017) .
- [10] Li, H., Li, X., and Luo, M., "Improving performance of differential pulse coding modulation based digital mobile fronthaul employing noise shaping," Opt. Express 26(9), 1407-11417 (2018).
- [11] Zhang, L., Pang, X., Ozolins, O., Udalcovs, A., Popov, S., Xiao, S. and Chen, J., "K-means Clustering based Multi-Dimensional Quantization Scheme for Digital Mobile Fronthaul," Proc. OFC, Th2A.51, (2018).
- [12] Zhang, L., Pang, X., Ozolins, O., Udalcovs, A., Popov, S., L. Wosinska, Hu, W., Xiao, S., and Chen, J., "Spectrally efficient digitized radio-over-fiber system with k-means clustering-based multidimensional quantization," Opt. Letters 43(7), 1546-1549 (2018).
- [13] Guo, B., Cao, W., Tao, A. and Samardzija, D., "LTE/LTE-A signal compression on the CPRI interface." Bell Labs Tech. J. 18(2), 117–133 (2013).
- [14] Udalcovs, A., Pang, X., Ozolins, O., Lin, R., Gan, L., Schatz, R., Djupsjöbacka, A., Mårtensson, J., Tang, M., Fu, S., Liu, D., Tong, W., Chen, J., Popov, S., and Jacobsen, G., "MCF-Enabled Self-Homodyne 16/64QAM Transmission for SDM Optical Access Networks," Proc. CLEO, SM4C.5, (2018).
- [15] Liu, X., Zeng, H., Chand, N., and Effenberger, F., "CPRI-compatible efficient mobile fronthaul transmission via equalized TDMA achieving 256 Gb/s CPRI-equivalent data rate in a single 10-GHz-bandwidth IM-DD channel," Proc. OFC, W1H.3, (2016).
- [16] Zhang, L., Udalcovs, A., Lin, R., Ozolins, O., Pang, X., Gan, L., Schatz, R., Tang, M., Fu, S., Liu, D., Tong, W., Popov, S., Jacobsen, G., Hu, W., Xiao, S. and Chen, J., "Towards Terabit Digital Radio over Fiber Systems: Architecture and Key Technologies," in IEEE Communications Magazine, to appear, (2018).